

Helicity modulus as renormalized coupling in the $O(3)$ σ -model



Heiko Molke¹ and Ulli Wolff
Institut für Physik, Humboldt Universität
Invalidenstr. 110, D-10099 Berlin, Germany

Abstract

For the family of $O(n)$ invariant nonlinear σ -models we consider boundary conditions that are periodic up to an $O(n)$ rotation. The helicity modulus is related to the change in free energy under variations of the corresponding angle. It defines a nonperturbative finite volume running coupling similar to the Schrödinger functional for QCD. For the two-dimensional $O(3)$ -model we investigate this quantity by analytical and numerical techniques. We establish its universal continuum relation to the finite volume massgap coupling at all scales and coupling strengths.

¹ Present address: DESY, Platanenallee 6, D-15738 Zeuthen

1 Introduction

The property of asymptotic freedom is a decisive feature of QCD as well as of a large class of two dimensional nonabelian spin models like the $O(n)$ σ -models for $n > 2$. Although it is based only on proofs in perturbation theory (to all orders), the following structural properties of these models are widely accepted and assumed here². The continuum limit is reached at vanishing bare coupling and a mass scale emerges in the renormalized continuum theory by dimensional transmutation. Many features associated with much higher energies or short distance can be related to each other by renormalized perturbation theory. Usually one singles out one suitable high energy quantity as renormalized coupling and constructs expansions for other observables in its powers. Other phenomena around the fundamental scale, like the spectrum, are not accessible to this strategy and are often investigated by numerical simulation. These opposite “sectors” are really features of one and the same theory and it is hence both interesting and possible to relate them, that is, to compute renormalized coupling constants at high energy in terms of the low energy scale. This has been the programme of the ALPHA collaboration in recent years. An efficient method has been developed first for the $O(3)$ σ -model [3] followed by quenched QCD which is reviewed in [4]. Many present activities are related to the goal of including dynamical quarks.

To relate the perturbative sector with low energy physics very dissimilar continuum scales have to be accommodated on a lattice with a spacing that is small compared to all other scales. In a direct approach this either calls for unmanageably large lattices or one has to compromise with the attempted limits like the continuum extrapolation. The ALPHA strategy overcomes this problem by a finite size scaling technique. A running coupling constant $\bar{g}^2(L)$ is constructed in the continuum limit, which at large L can be related to spectral scales and which at small L can be used as an expansion parameter and thus gives access to the perturbative sector. Step by step one computes $\bar{g}^2(2L)$ in terms of $\bar{g}^2(L)$ by continuum extrapolation. Since the system size L is used as the physical scale, L/a is the only large scale ratio, where a is the lattice spacing. The choice of \bar{g} is not unique and a number of practical criteria were taken into account.

² See ref. [2] for a diverging point of view

For the $O(n)$ model the finite volume mass gap was used in [3]

$$\bar{g}^2 = \frac{2}{n-1} m(L)L, \quad (1.1)$$

where $m(L)$ is the gap of the transfer matrix referring to spatial periodic boundary conditions with periodicity L . For $L \rightarrow \infty$, $m(L)$ saturates to the infinite volume massgap, which we identify with the dynamically generated scale. At small L the mass gap becomes perturbative [5] and can be used as an expansion parameter. For gauge theories a similarly convenient though less obvious quantity was defined via the Schrödinger functional [6, 4]. The basic mechanism is to study the response of the free energy under the variation of an angle that enters into non-trivial boundary conditions. Again the system size is the only scale beside the cutoff, and for the quenched theory α_s in the high energy limit has been computed to a satisfactory precision.

In this article we define and investigate an alternative coupling $g_{\Upsilon}(L)$ for the $O(n)$ σ -model in two dimensions, which is closely related to the helicity modulus. We compare its properties with the massgap coupling $\bar{g}(L)$. They can be analytically related in the continuum for both small and large coupling. Both expansions are checked and the crossover range is controlled by high precision numerical simulations. In the next section we define the helicity modulus and relate it to \bar{g} at strong coupling. In section 3 g_{Υ} is properly normalized and its weak coupling behavior is explored up to two loops with details given in appendix A. Section 4 summarizes our numerical work and gives conclusions. This work is based on the diploma thesis [1] of H. Molke. The introduction of g_{Υ} goes back to earlier attempts [7, 8] to investigate renormalization by finite size techniques.

2 Helicity modulus and transfer matrix

In this section we introduce the helicity modulus. For earlier discussions of similar quantities see Ref. [9] and further references found there.

We consider the $O(n)$ σ -model with its standard nearest neighbor lattice action

$$S = -\frac{1}{g_0^2} \sum_{x\mu} s(x)s(x+a\hat{\mu}), \quad (2.1)$$

where $s(x)$ is the unit length spin field and $\hat{\mu}, \mu = 0, 1$, are unit vectors along the axes of a square lattice with spacing a . We take T as the size in the time

or 0-direction and L in the other direction. In space direction we impose strictly periodic boundary conditions, while in the time direction we demand periodicity up to a planar $\text{SO}(n)$ rotation in spin space by an angle α ,

$$s(x + T\hat{0}) = \exp(\alpha K_{ij})s(x). \quad (2.2)$$

Here K_{ij} generates rotations in the ij plane,

$$(K_{ij})_{kl} = \delta_{ik}\delta_{jl} - \delta_{il}\delta_{jk}. \quad (2.3)$$

Integration of all spins with the $\text{O}(n)$ invariant measure gives the partition function

$$Z_\alpha = \int Ds \exp(-S). \quad (2.4)$$

Ratios $Z_{\alpha_1}/Z_{\alpha_2}$ depend on differences in free energy for different boundary conditions and are expected to be universal. We now define the helicity modulus Υ by

$$\Upsilon = -\frac{1}{Z_0} \left. \frac{\partial^2 Z_\alpha}{\partial \alpha^2} \right|_{\alpha=0}. \quad (2.5)$$

From this definition it is rather easy to establish a connection between Υ and the transfer matrix \mathcal{T} . For the fully periodic case Z_0 we have

$$Z_0 = \text{tr}[\mathcal{T}^{T/a}]. \quad (2.6)$$

The extra twist by an angle α corresponds to inserting a rotation operator under the trace in the Hilbert space where \mathcal{T} operates,

$$Z_\alpha = \text{tr}[\mathcal{T}^{T/a} \exp(i\alpha \mathcal{K}_{ij})]. \quad (2.7)$$

If we realize states as wavefunctions $\psi(\sigma)$ on spatial one dimensional spin fields σ , this induced operator is given by

$$(\exp(i\alpha \mathcal{K}_{ij})\psi)(\sigma) = \psi(\exp(-\alpha K_{ij})\sigma). \quad (2.8)$$

The operator \mathcal{T} possesses real positive eigenvalues $\lambda_0 > \lambda_1 \geq \lambda_2 \geq \dots$ with λ_0 corresponding to the nondegenerate ground state. These eigenvalues depend on L and a . We define the massgap $m(L)$ as

$$\exp(-m(L)a) = \frac{\lambda_1}{\lambda_0}. \quad (2.9)$$

Due to the $O(n)$ invariance \mathcal{T} and \mathcal{K}_{ij} commute and we simultaneously diagonalize the generator that appears in (2.7). So for each eigenstate there is a value $m_k, k = 0, 1, 2, \dots$. For $n = 3$ these are just the “magnetic” quantum numbers of eigenstates in all possible integer isospin multiplets in the spectrum. The α -dependent partition function is now given by

$$Z_\alpha = \sum_{k \geq 0} (\lambda_k)^{T/a} \exp(i\alpha m_k), \quad (2.10)$$

and for the helicity modulus we obtain

$$\Upsilon = \frac{1}{Z_0} \sum_{k \geq 0} (\lambda_k)^{T/a} m_k^2. \quad (2.11)$$

For large T we expect the ground state and the lowest excitations above it to dominate. While the ground state is $O(n)$ invariant, $m_0 = 0$, we expect an n -fold degenerate vector multiplet as the next excitations above it. On it the generators are represented in the form (2.3) and have eigenvalues 1, -1 and $n - 2$ times 0. Asymptotically this implies

$$\Upsilon \stackrel{T \rightarrow \infty}{\simeq} 2 \exp(-m(L)T) [1 + O(\exp(-m^*T))], \quad (2.12)$$

where m^* is either $m(L)$ or the gap between the vector multiplet and the next state with nonsinglet $O(n)$ behavior, depending on which gap is smaller. We work at fixed aspect ratio

$$\rho = \frac{T}{L}, \quad (2.13)$$

and Υ is given in terms of the renormalized coupling (1.1) introduced in [3] by

$$\Upsilon(L) \stackrel{\bar{g}^2 \rightarrow \infty}{\simeq} 2 \exp\left(-\frac{n-1}{2} \rho \bar{g}^2(L)\right). \quad (2.14)$$

This asymptotic formula holds for any value of the lattice spacing and hence in the continuum limit.

3 Helicity modulus in perturbation theory

3.1 Preparation and leading order

By changing the integration variables in (2.4)

$$s(x) \rightarrow \exp\left(-\alpha \frac{x_0}{T} K_{ij}\right) s(x) \quad (3.1)$$

we arrive at

$$Z_\alpha = \int Ds \exp(-S_B) \quad (3.2)$$

where the action

$$S_B = -\frac{1}{g_0^2} \sum_{x\mu} s(x) B_\mu s(x + a\hat{\mu}) \quad (3.3)$$

has acquired a constant $\text{SO}(n)$ gauge field

$$B_0 = \exp\left(\alpha \frac{a}{T} K_{ij}\right), \quad B_1 = 1, \quad (3.4)$$

and $s(x)$ has become strictly periodic. The helicity modulus is now expressed by an expectation value in the periodic ensemble

$$\Upsilon = \left\langle \frac{\partial^2 S_B}{\partial \alpha^2} - \left(\frac{\partial S_B}{\partial \alpha} \right)^2 \right\rangle \quad (3.5)$$

with $B_\mu = 1$ after taking all derivatives. So far the angle α has referred to rotations with one particular generator K_{ij} . At this point we average over all planes $i < j$ and split Υ into two $\text{O}(n)$ invariant contributions $\Upsilon = \Upsilon_1 - \Upsilon_2$,

$$\Upsilon_1 = \left\langle \frac{\partial^2 S_B}{\partial \alpha^2} \right\rangle = \frac{2}{n\rho g_0^2} \frac{a^2}{V} \sum_x \langle s(x) s(x + a\hat{0}) \rangle \quad (3.6)$$

and

$$\Upsilon_2 = \left\langle \left(\frac{\partial S_B}{\partial \alpha} \right)^2 \right\rangle = \frac{2}{n(n-1)\rho g_0^4} \frac{a^4}{V} \sum_{i < j} \sum_{xy} \langle j_{ij}^0(x) j_{ij}^0(y) \rangle. \quad (3.7)$$

In these expressions the volume $V = TL$ and the currents

$$j_{ij}^\mu(x) = s(x) K_{ij} \Delta_\mu s(x) \quad (3.8)$$

with the discrete derivative

$$\Delta_\mu s(x) = \frac{1}{a} [s(x + a\hat{\mu}) - s(x)] \quad (3.9)$$

have been introduced. While Υ_1 is a nearest neighbor correlation essentially corresponding to the internal energy, Υ_2 is a kind of susceptibility with correlations over all separations. In perturbation theory contributions to Υ_2 start at one loop level and we find to leading order in g_0

$$\Upsilon = \frac{2}{n\rho g_0^2} + \text{O}(1). \quad (3.10)$$

A correctly normalized and nonperturbatively defined renormalized L -dependent coupling constant can now be defined as

$$g_{\Upsilon}^2 = \frac{2}{n\rho} \frac{1}{\Upsilon}, \quad (3.11)$$

quite in the spirit of the Schrödinger functional. Its relation to \bar{g} from ref.[3] is

$$g_{\Upsilon}^2 = \begin{cases} \bar{g}^2 + \mathcal{O}(\bar{g}^4) & \text{for } \bar{g}^2 \rightarrow 0 \\ \frac{1}{n\rho} \exp\left(\frac{n-1}{2}\rho\bar{g}^2\right) & \text{for } \bar{g}^2 \rightarrow \infty. \end{cases} \quad (3.12)$$

As \bar{g}^2 is proportional to L at large volume or strong coupling, we find exponential growth for g_{Υ}^2 . This is also expected for the Schrödinger functional coupling in gauge theory [10]. The origin in both cases is the exponentially small sensitivity of the free energy to boundary effects in a physically large volume.

3.2 Results of a two loop calculation

For simplicity we confined ourselves to the case $T = L, \rho = 1$ for our perturbative and our numerical calculations. Details on the perturbative evaluation of Υ are given in appendix A. Nontrivial coefficients were evaluated for sequences of lattices of finite L/a and then fitted to the expected asymptotic form. The extrapolation was carried out as described in appendix D of ref. [11] with lattices up to $L/a = 100$. The cost in CPU time was negligible in this two dimensional case. As for the Schrödinger functional, it was advantageous to compute some of the two loop diagrams in position space rather than momentum space.

The nearest neighbor correlation in Υ_1 is rather simple to compute [12] to the required order. As a result we find

$$\Upsilon_1 = \frac{2}{n} \frac{1}{g_0^2} - \frac{n-1}{2n} - \frac{n-1}{16n} g_0^2 + \mathcal{O}(g_0^4, a^2). \quad (3.13)$$

The current-current correlation in Υ_2 is more involved and has the structure

$$\Upsilon_2 = \Upsilon_2^{(0)} + \Upsilon_2^{(1)} g_0^2 + \mathcal{O}(g_0^4). \quad (3.14)$$

By combining the results for $\Upsilon_2^{(0)}$ and $\Upsilon_2^{(1)}$ from the appendix with the expansion of \bar{g}^2 on the lattice [3, 15] we find in the continuum limit the

renormalized perturbative series

$$g_{\Upsilon}^2(L) = \bar{g}^2(sL) + d_1 \bar{g}^4(sL) + d_2 \bar{g}^6(sL) + \mathcal{O}(\bar{g}^8(sL)) \quad (3.15)$$

with

$$d_1(s) = (n-2) 0.16350689821 - \frac{1}{2\pi} \ln s \quad (3.16)$$

$$d_2(s) = d_1(s)^2 + (n-2) [0.00315826256 - (n-2) 0.007733893180] - \frac{1}{(2\pi)^2} \ln s. \quad (3.17)$$

Note that a free relative factor s between the scales at which g_{Υ} and \bar{g} are taken has been introduced here for later use.

4 Numerical results

Our main goal in this section is to establish the nonperturbative relation between $\bar{g}^2(L)$ and $g_{\Upsilon}^2(L)$ in the continuum limit of the $O(3)$ model for arbitrary values of these couplings. Our strategy is to first construct series of values L/a and $\beta = 1/g_0^2$ which correspond to fixed values of \bar{g} . For precisely the same series we measure g_{Υ}^2 and extrapolate these values to $L/a \rightarrow \infty$. For the first part of the task we include but extend as necessary the data from [3]. These runs were carried out with precisely the same code as described there. In particular, we took advantage of free boundary conditions in the time direction to extract the massgap, and the reweighting technique allowed for a post-run fine-tuning of β to match a desired value of \bar{g}^2 . The simulation of Υ is rather conventional on an $L \times L$ torus. We employed the single cluster algorithm [13] and measured the observables given in eqs. (3.6) and (3.7). Both kinds of results are collected in Table 1.

For each of the eight series at fixed \bar{g}^2 we have pairs of values with errors δ of \bar{g}^2 and (δ_{Υ}) of g_{Υ}^2 . For the extrapolation in a/L we combine them into effective errors in g_{Υ}^2 only

$$\Delta(g_{\Upsilon}^2) = \sqrt{\delta_{\Upsilon}^2 + \left(\frac{\partial g_{\Upsilon}^2}{\partial \bar{g}^2} \delta \right)^2}. \quad (4.1)$$

The required slope can be estimated with sufficient accuracy from the weak and strong coupling behavior. We then extrapolate by fitting a function

L	β	\bar{g}^2	g_{Υ}^2	β	\bar{g}^2	g_{Υ}^2
6				1.8439	0.8166(5)	0.9108(2)
8				1.8947	0.8166(4)	0.9210(2)
10	2.0489	0.7390(5)	0.8276(1)	1.9319	0.8166(6)	0.9276(2)
12				1.9637	0.8166(6)	0.9295(2)
16	2.1260	0.7390(6)	0.8341(1)	2.0100	0.8166(5)	0.9350(2)
20	2.1626	0.7390(5)	0.8361(1)	2.0489	0.8166(8)	0.9351(2)
24	2.1930	0.7390(6)	0.8369(1)			
32	2.2422	0.7390(5)	0.8363(1)	2.1260	0.8166(8)	0.9375(3)
6	1.7276	0.9176(6)	1.0327(3)	1.6050	1.0595(7)	1.2063(4)
8	1.7791	0.9176(5)	1.0460(3)	1.6589	1.0595(7)	1.2276(4)
10	1.8171	0.9176(6)	1.0551(3)	1.6982	1.0595(7)	1.2414(4)
12	1.8497	0.9176(7)	1.0587(3)	1.7306	1.0595(7)	1.2462(4)
16	1.8965	0.9176(5)	1.0642(3)	1.7800	1.0595(6)	1.2541(4)
20				1.8171	1.0595(7)	1.2579(4)
24	1.9637	0.9176(6)	1.0674(3)			
10	1.3634	2.0373(18)	2.9635(12)	1.2939	2.4596(16)	4.268(2)
12	1.4060	2.0373(18)	2.9848(12)	1.3413	2.4596(16)	4.284(3)
16	1.4683	2.0373(18)	3.0120(12)	1.4095	2.4596(17)	4.302(3)
20				1.4579	2.4596(17)	4.316(3)
24	1.5470	2.0373(18)	3.0283(13)	1.4948	2.4596(17)	4.337(3)
32	1.6000	2.0373(18)	3.0314(18)	1.5500	2.4596(16)	4.344(3)
10	1.2211	3.0280(27)	7.022(6)	1.1427	3.7692(17)	13.947(8)
12	1.2736	3.0280(27)	7.076(7)	1.2014	3.7692(19)	14.030(8)
16	1.3481	3.0280(27)	7.140(7)	1.2847	3.7692(18)	14.106(9)
24	1.4413	3.0280(27)	7.158(8)	1.3862	3.7692(17)	14.179(11)
32	1.5000	3.0280(27)	7.208(8)	1.4500	3.7692(16)	14.218(11)

Table 1: Simulation results for \bar{g}^2 and g_{Υ}^2 .

$A + B(a/L)^2$ to the g_{Υ}^2 values with these errors. A typical case is shown in Fig. 1 and an acceptable fit was achieved in all cases. Our extrapolated continuum results are collected in Table 2. They are plotted in Fig. 2 and the close-up in Fig. 3, where one sees the data branch off from the 2-loop curve (3.15). After a very narrow transition region they follow the strong coupling behavior in (3.12).

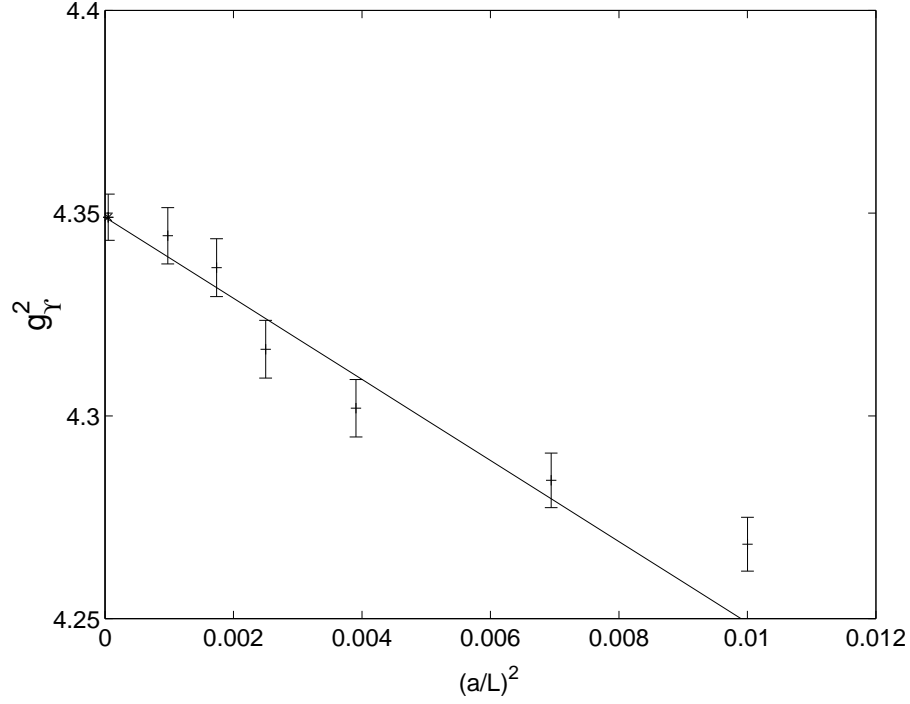


Figure 1: Continuum extrapolation of g_Y^2 for $\bar{g}^2 = 2.4596$ as a typical example.

\bar{g}^2	g_Y^2
0.7390	0.8388(6)
0.8166	0.9386(6)
0.9176	1.0701(7)
1.0595	1.2631(9)
2.0373	3.0407(33)
2.4596	4.349(6)
3.0280	7.210(15)
3.7692	14.234(20)

Table 2: Nonperturbative relation between \bar{g}^2 and g_Y^2 .

To get a feeling for the lattice artefacts associated with our two couplings individually we estimated their step scaling function (SSF) for a pair of values

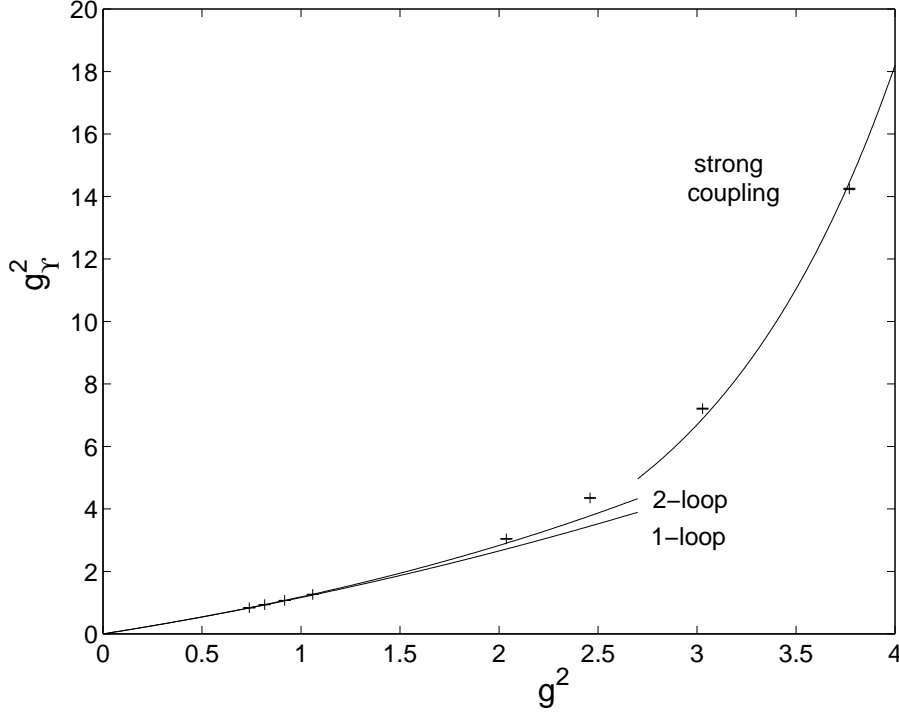


Figure 2: Coupling g_Y^2 versus \bar{g}^2 with asymptotic expansions.

corresponding to similar L , $\bar{g}^2 \approx 1.06$ and $g_Y^2 \approx 1.29$. The SSF — the focus of interest in [3] — gives $\bar{g}^2(2L)$ as a function of $\bar{g}^2(L)$. Pairs of simulations at identical β and sizes L/a and $2L/a$ yield

$$\Sigma(u, a/L) = \bar{g}^2(2L) \Big|_{\bar{g}^2(L)=u} . \quad (4.2)$$

Σ is then extrapolated to the continuum limit. A completely analogous quantity Σ_Y is defined in terms of g_Y^2 . In Fig. 4 the continuum approaches of Σ and Σ_Y are shown. Lattice artefacts amount to a few percent at say $L/a = 8$ with Σ_Y deviating significantly more from its continuum limit than Σ . This trend is expected, since Y receives contributions from several low-lying eigenstates of the transfer matrix (c.f. (2.11)) while \bar{g} is constructed in terms of the massgap only.

Instead of relating the two couplings at one scale L one may also consider the connection between $g_Y^2(L)$ and $\bar{g}^2(sL)$. This has already been incorporated in the perturbative formulas (3.15). One may hope that an appropriate

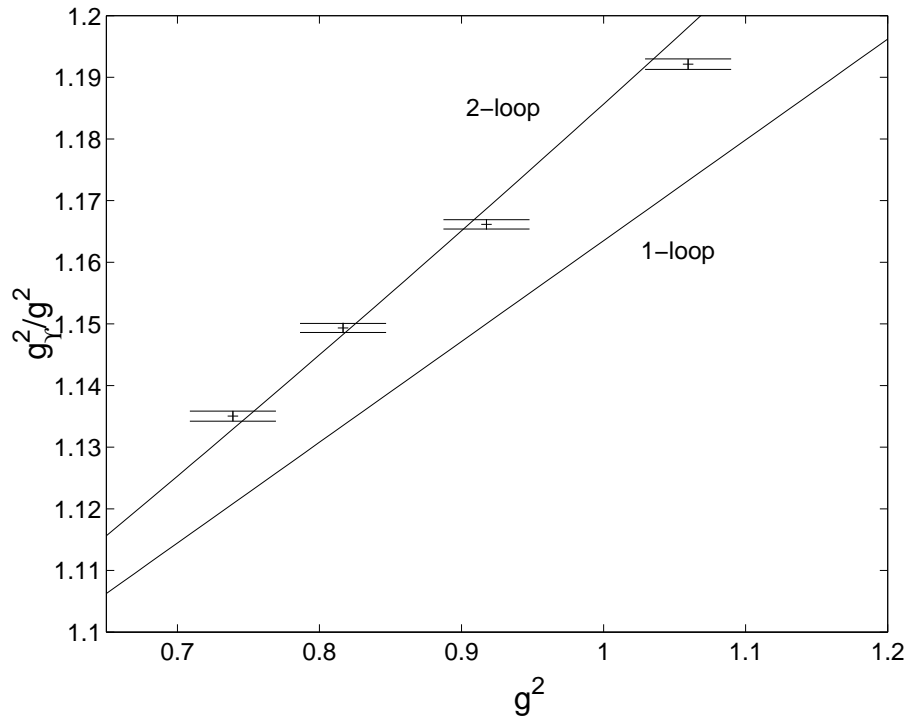


Figure 3: Close-up of g_Y^2/\bar{g}^2 in the transition region.

choice of s improves the accuracy of the approximation as was for instance found in [10]. A somewhat natural value is $s = 2.7936$ ($n = 3$), for which $d_1(s)$ in (3.16) vanishes and which coincides with the ratio of the Λ -parameters associated with the short distance behaviors of the two couplings. To compare such an expansion with non-perturbative results we would have to simulate series of lattices of size L and sL at the same bare couplings and take the continuum limit. While this is not possible, we gained good control over the step scaling function for $\bar{g}^2(L)$ in [3]. We used its four loop approximation [15, 16]³ and fitted the remainder with an effective five loop coefficient to evolve from $\bar{g}^2(L)$ to $\bar{g}^2(sL)$. In this way we found however no value $s \neq 1$ which significantly improved the series for $g_Y^2(L)$.

To conclude, we have investigated two nonperturbatively defined coupling constants for the $O(3)$ nonlinear σ -model with exponentially different

³ We evaluated $\tilde{b}_4 = 0.0040$ at $n = 3$ for eq.(3.47) in [16].

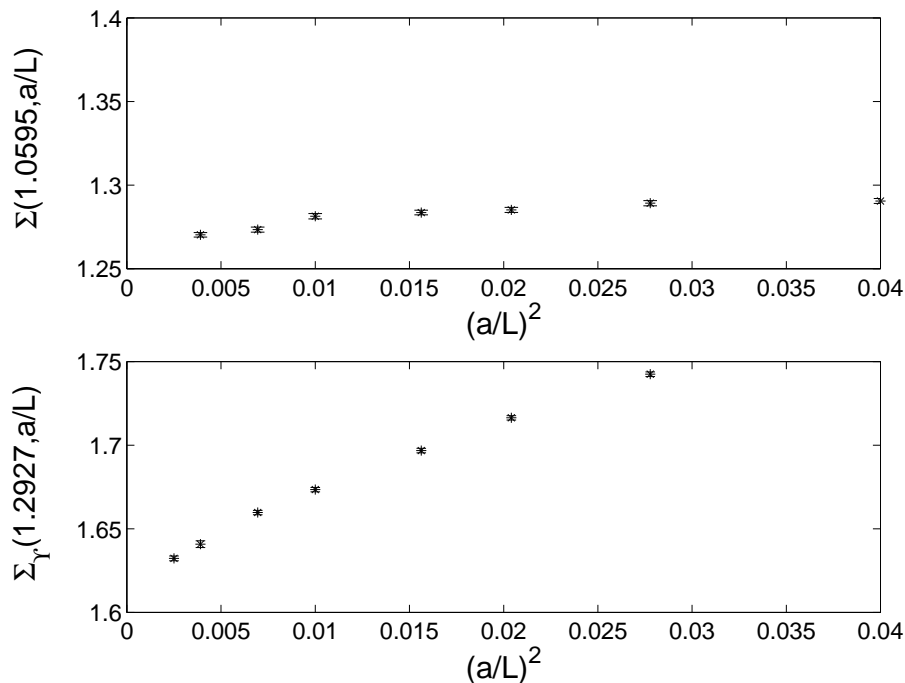


Figure 4: Continuum approach of step scaling functions.

low energy behaviors. Analytical relations, valid in the continuum limit, are available for both weak and strong coupling. Precise numerical simulations covered the intermediate range and matched with both asymptotic expansions. As expected, the helicity modulus coupling shows larger lattice artefacts than the finite volume massgap.

A Two loop expansion of Υ

In this appendix we use lattice units with $a = 1$ and take $T = L$. For the perturbative expansion of the σ -model on a finite lattice we have to fix the global $O(n)$ invariance by the Fadeev-Popov technique [14]. For $O(n)$ invariant integrands $I(s)$ it amounts to the replacement $I(s) \rightarrow I(s)f(s)F(s)$ which does not change the value of the integral. For the noninvariant function f we take

$$f(s) = \delta(M_1)\delta(M_2)\cdots\delta(M_{n-1}) \quad (\text{A.1})$$

where $M = \sum_x s(x)$ is the total magnetization, which is hence forced to point in the n -direction. The compensating Fadeev-Popov factor is in this case given by

$$F(s) = |M|^{n-1} \quad (\text{A.2})$$

up to an irrelevant overall constant factor. The spins are parameterized by an $n - 1$ component real field $\phi(x)$

$$s = (g_0 \phi, \chi), \quad \chi = \sqrt{1 - g_0^2 \phi^2}. \quad (\text{A.3})$$

The resulting contributions are gathered in an effective action

$$S_{\text{eff.}} = \frac{1}{2} \sum_{x\mu} \left[(\Delta_\mu \phi)^2 + \frac{1}{g_0^2} (\Delta_\mu \chi)^2 \right] + \sum_x \ln \chi - (n - 1) \ln \left(\sum_x \chi \right). \quad (\text{A.4})$$

It is understood to be expanded in g_0 ,

$$S_{\text{eff.}} = \sum_{k=0}^{\infty} g_0^{2k} S^{(k)}, \quad (\text{A.5})$$

and the function f still has to be included in the path integral. It leads to the omission of the zero momentum mode in the propagator of the ϕ field and makes perturbative coefficients now well defined. The last two terms in $S_{\text{eff.}}$ correspond to the $O(n)$ invariant measure and to F . We shall only need the leading terms

$$S^{(0)} = \frac{1}{2} \sum_x (\Delta_\mu \phi)^2 \quad (\text{A.6})$$

$$S^{(1)} = \frac{1}{8} \sum_x (\Delta_\mu \phi^2)^2 - \frac{1}{2} \left(1 - (n - 1) \frac{1}{V} \right) \sum_x \phi^2. \quad (\text{A.7})$$

The term $S^{(0)}$ defines the propagator

$$\langle \phi_k(x) \phi_l(y) \rangle_0 = \delta_{kl} G(x - y) = \delta_{kl} \frac{1}{V} \sum'_p \frac{e^{ip(x-y)}}{\hat{p}^2} \quad (\text{A.8})$$

where $1 \leq k, l \leq n - 1$ and the primed sum is over the appropriate lattice momenta excluding $p = (0, 0)$ and we have introduced $\hat{p}_\mu = 2 \sin(p_\mu/2)$.

To compute Υ_1 we set

$$s(x)s(x+a\hat{0}) = 1 - g_0^2 E^{(0)} - g_0^4 E^{(1)} + O(g_0^6) \quad (\text{A.9})$$

$$E^{(0)} = \frac{1}{2}(\Delta_0 \phi)^2 \quad (\text{A.10})$$

$$E^{(1)} = \frac{1}{8}(\Delta_0 \phi^2)^2 \quad (\text{A.11})$$

and find

$$\Upsilon_1 = \frac{2}{ng_0^2} \left(1 - g_0^2 \langle E^{(0)} \rangle_0 - g_0^4 \left[\langle E^{(1)} \rangle_0 - \langle E^{(0)} S^{(1)} \rangle_0^c \right] \right) \quad (\text{A.12})$$

with the connected correlation in the last bracket. These contributions evaluate to

$$\langle E^{(0)} \rangle_0 = \frac{n-1}{4} \left(1 - \frac{1}{L^2} \right) \quad (\text{A.13})$$

$$\langle E^{(1)} \rangle_0 - \langle E^{(0)} S^{(1)} \rangle_0^c = \frac{n-1}{32} \left(1 - \frac{1}{L^2} \right)^2 - \frac{(n-1)(n-2)}{4} A_1 \frac{1}{L^2}. \quad (\text{A.14})$$

The contribution Υ_2 has been expanded in (3.14). We introduce

$$\frac{1}{Vg_0^4} \sum_{i < j} \sum_{xy} j_{ij}^0(x) j_{ij}^0(y) = H^{(0)} + g_0^2 H^{(1)} + O(g_0^4) \quad (\text{A.15})$$

$$H^{(0)} = \frac{4}{V} \sum_{k < l} \left(\sum_x \phi_k \bar{\Delta}_0 \phi_l \right)^2 \quad (\text{A.16})$$

$$H^{(1)} = \frac{1}{V} \sum_k \left(\sum_x \phi^2 \bar{\Delta}_0 \phi_k \right)^2 \quad (\text{A.17})$$

with the symmetric derivative

$$\bar{\Delta}_\mu \phi(x) = \frac{1}{2} [\phi(x + \hat{\mu}) - \phi(x - \hat{\mu})] \quad (\text{A.18})$$

and find

$$\Upsilon_2 = \frac{2}{n(n-1)} \left(\langle H^{(0)} \rangle_0 + g_0^2 \left[\langle H^{(1)} \rangle_0 - \langle H^{(0)} S^{(1)} \rangle_0^c \right] \right). \quad (\text{A.19})$$

Numerical values are

$$\langle H^{(0)} \rangle_0 = (n-1)(n-2)(A_1 - \frac{1}{4}A_2) \quad (\text{A.20})$$

$$\langle H^{(1)} \rangle_0 = (n-1)[(n-2)B_1 + B_2] \quad (\text{A.21})$$

$$\begin{aligned} \langle H^{(0)} S^{(1)} \rangle_0^c &= (n-1)(n-2) \left[(A_1 - \frac{1}{4}A_2)(A_1 + \frac{1}{4}A_2 - \frac{1}{2}(1 - \frac{1}{V})) \right. \\ &\quad \left. + 2 \frac{n-2}{V} A_3 \right] \end{aligned} \quad (\text{A.22})$$

In the above expressions the following L -dependent constants were introduced,

$$A_1 = \frac{1}{V} \sum_p' \frac{1}{\hat{p}^2} \quad (\text{A.23})$$

$$A_2 = \frac{1}{V} \sum_p' \frac{\sum_\mu \hat{p}_\mu^4}{(\hat{p}^2)^2} \quad (\text{A.24})$$

$$A_3 = \frac{1}{V} \sum_p' \frac{\sum_\mu \sin^2(p_\mu)}{(\hat{p}^2)^3} \quad (\text{A.25})$$

$$B_1 = - \sum_{x\mu} G(x)^2 \bar{\Delta}_\mu \bar{\Delta}_\mu G(x) \quad (\text{A.26})$$

$$B_2 = B_1 - 2 \sum_{x\mu} G(x) [\bar{\Delta}_\mu G(x)]^2. \quad (\text{A.27})$$

Evaluated as x - or p -sums as they stand, only $O(V)$ terms have to be summed.

It is now straightforward to express the coefficients k_1, k_2 in

$$g_{\Upsilon}^2 = \frac{2}{n\Upsilon} = g_0^2 + k_1 g_0^4 + k_2 g_0^6 + O(g_0^8) \quad (\text{A.28})$$

in terms of the above constants. We evaluated them numerically for $L = 8 \dots 100$ and determined the asymptotic behavior as explained in the appendix of Ref. [11]. The result is

$$k_1 = (n-2) \left[\frac{\ln(L)}{2\pi} - 0.12165689529 \right] + \frac{n-1}{4} + O(1/L^2) \quad (\text{A.29})$$

$$\begin{aligned} k_2 - k_1^2 &= (n-2) \left[\frac{\ln(L)}{(2\pi)^2} + 0.02514054821 \right] \\ &\quad - (n-2)^2 0.00773389318 + \frac{5}{96} + O(1/L^2) \end{aligned} \quad (\text{A.30})$$

Errors are beyond the digits given here, and the coefficients of $\ln(L)/L^2$ and $1/L^2$ corrections are also known but not listed here. They are of the same size as the constants appearing here. To obtain the last fraction we set $B_2 = 1/48 + O(1/L^2)$ which we observed to very high accuracy.

The massgap coupling (1.1) has been computed perturbatively up to two loops in [3] and to three loops in [15, 16]. From the last reference we extract

$$\bar{g}^2 = g_0^2 + m_1 g_0^4 + m_2 g_0^6 + O(g_0^8) \quad (\text{A.31})$$

with

$$m_1 = (n-2) \left[\frac{\ln(L)}{2\pi} + \frac{\ln(\sqrt{2}/\pi) + \gamma}{2\pi} \right] + \frac{1}{4} + O(1/L^2) \quad (\text{A.32})$$

$$m_2 - m_1^2 = (n-2) \left[\frac{\ln(L)}{(2\pi)^2} + 0.021982285645 \right] + \frac{5}{96} + O(1/L^2) \quad (\text{A.33})$$

The exact fraction was again found to numerical precision.

References

- [1] H. Molke, “Renormierte Kopplungen im $O(3)$ σ -Modell”
Diploma Thesis, Humboldt University, Berlin, May 2000,
[http://dochoost.rz.hu-berlin.de/
diplom/physik/molke-heiko-2000-05-02/PS/Molke.ps](http://dochoost.rz.hu-berlin.de/diplom/physik/molke-heiko-2000-05-02/PS/Molke.ps)
- [2] A. Patrascioiu and E. Seiler, hep-lat/0009005.
- [3] M. Lüscher, P. Weisz and U. Wolff, Nucl. Phys. **B359**, 221 (1991).
- [4] R. Sommer [ALPHA Collaboration], Lectures given at 36. Internationale
Universitätswochen für Kern- und Teilchenphysik, Schladming 1997,
hep-ph/9711243.
- [5] M. Lüscher, Phys. Lett. **B118**, 391 (1982).
- [6] M. Lüscher, R. Narayanan, P. Weisz and U. Wolff, Nucl. Phys. **B384**,
168 (1992) [hep-lat/9207009].
- [7] U. Wolff, Nucl. Phys. **B265**, 506 (1986).
- [8] U. Wolff, Nucl. Phys. **B265**, 537 (1986).
- [9] N. Schultka, cond-mat/9611043.
S. Chakravarty, Phys. Rev. **66**, 481 (1990).
- [10] G. de Divitiis *et al.* [Alpha Collaboration], Nucl. Phys. **B437**, 447 (1995)
[hep-lat/9411017].
- [11] A. Bode, P. Weisz and U. Wolff [ALPHA collaboration], Nucl. Phys.
B576, 517 (2000) [hep-lat/9911018].
- [12] B. Alles, A. Buonanno and G. Cella, Nucl. Phys. **B500**, 513 (1997)
[hep-lat/9701001].
- [13] U. Wolff, Phys. Rev. Lett. **62**, 361 (1989).
- [14] P. Hasenfratz, Phys. Lett. **B141**, 385 (1984).
- [15] D. Shin, Nucl. Phys. **B496**, 408 (1997) [hep-lat/9611006].
- [16] D. Shin, Nucl. Phys. **B546**, 669 (1999) [hep-lat/9810025].